JVI Journals.ASM.org

Herpesvirus saimiri MicroRNAs Preferentially Target Host Cell Cycle Regulators

Yang Eric Guo,* Theresa Oei, Joan A. Steitz

Department of Molecular Biophysics and Biochemistry, Howard Hughes Medical Institute, Yale School of Medicine, New Haven, Connecticut, USA

ABSTRACT

In latently infected marmoset T cells, *Herpesvirus saimiri* (HVS) expresses six microRNAs (known as miR-HSURs [*H. saimiri* U-rich RNAs]). The viral miR-HSURs are processed from chimeric primary transcripts, each containing a noncoding U-rich RNA (HSUR) and a pre-miRNA hairpin. To uncover the functions of miR-HSURs, we identified mRNA targets in infected cells using high-throughput sequencing of RNA isolated by cross-linking immunoprecipitation (HITS-CLIP). HITS-CLIP revealed hundreds of robust Argonaute (Ago) binding sites mediated by miR-HSURs that map to the host genome but few in the HVS genome. Gene ontology analysis showed that several pathways regulating the cell cycle are enriched among cellular targets of miR-HSURs. Interestingly, miR-HSUR4-3p represses expression of the p300 transcriptional coactivator by binding the open reading frame of its mRNA. miR-HSUR5-3p directly regulates BiP, an endoplasmic reticulum (ER)-localized chaperone facilitating maturation of major histocompatibility complex class I (MHC-I) and the antiviral response. miR-HSUR5-3p also robustly downregulates WEE1, a key negative regulator of cell cycle progression, leading to reduced phosphorylation of its substrate, cyclin-dependent kinase (Cdk1). Consistently, inhibition of miR-HSUR5-3p in HVS-infected cells decreases their proliferation. Together, our results shed light on the roles of viral miRNAs in cellular transformation and viral latency.

IMPORTANCE

Viruses express miRNAs during various stages of infection, suggesting that viral miRNAs play critical roles in the viral life cycle. Compared to protein-coding genes, the functions of viral miRNAs are not well understood. This is because it has been challenging to identify their mRNA targets. Here, we focused on the functions of the recently discovered HVS miRNAs, called miR-HSURs. HVS is an oncogenic gammaherpesvirus that causes acute T-cell lymphomas and leukemias in New World primates and transforms human T cells. A better understanding of HVS biology will help advance our knowledge of virus-induced oncogenesis. Because numerous cellular miRNAs play crucial roles in cancer, viral miRNAs from the highly oncogenic HVS might also be important for transformation. Here, we found that the miR-HSURs preferentially modulate expression of host cell cycle regulators, as well as antiviral response factors. Our work provides further insight into the functions of herpesviral miRNAs in virus-induced oncogenesis and latency.

Herpesvirus saimiri (HVS) is a T-lymphotropic gammaherpesvirus that causes acute T-cell lymphomas and leukemias in New World primates and transforms human primary T cells *in vitro* (1). The most abundant transcripts in HVS latently infected marmoset T cells are seven noncoding U-rich RNAs, known as HSURs (*H. saimiri* U-rich RNAs) (2). The functions of these viral noncoding RNAs are not well understood. HSUR1 forms base-pairing interactions with a host microRNA (miRNA), miR-27, targeting it for rapid degradation (3). This helps to promote constitutive activation of infected T cells and viral latency (4, 5). We recently discovered that, in addition to the HSURs, HVS expresses during latency another class of noncoding RNAs: six miRNAs called miR-HSURs (6). The miR-HSURs are cotranscribed together with the HSURs to give rise to chimeric primary transcripts, which are then processed via a combination of canonical and noncanonical pathways to yield mature HSURs and miRNAs (6).

In complex with Argonaute (Ago) family proteins, mature miRNAs modulate target protein levels through base pairing with their mRNAs (7). Like cellular miRNAs, viral miRNAs play key regulatory roles in gene expression in host cells (8). Previous studies suggested that viral miRNAs benefit infection and the viral life cycle through regulation of (i) viral persistence, (ii) proliferation and/or survival of the infected host cells, and (iii) host immune evasion (2). Because the functions of the miR-HSURs were unknown, we embarked on the identification of their viral and cellular targets in latently infected marmoset T cells.

MATERIALS AND METHODS

Cell culture and transfection. Marmoset (*Callithrix jacchus*) T cells infected with HVS strain Δ2A (referred to as Δ2A cells) were generated and grown as described previously (9). They were derived from marmoset peripheral blood lymphocytes immortalized by HVS and are predominantly activated CD8 cytotoxic T cells. A 1,379-bp deletion present in the

Received 26 July 2015 **Accepted** 12 August 2015

Accepted manuscript posted online 19 August 2015

Citation Guo YE, Oei T, Steitz JA. 2015. *Herpesvirus saimiri* microRNAs preferentially target host cell cycle regulators. J Virol 89:10901–10911. doi:10.1128/JVI.01884-15.

Editor: R. M. Sandri-Goldin

Address correspondence to Joan A. Steitz, joan.steitz@yale.edu.

* Present address: Yang Eric Guo, Whitehead Institute for Biomedical Research, Cambridge, MA, USA.

Supplemental material for this article may be found at http://dx.doi.org/10.1128/JVI.01884-15.

genome of strain Δ2A eliminated expression of HSUR1, HSUR2, miR-HSUR2-5p, and miR-HSUR2-3p. Previously, we generated high-quality Ago high-throughput sequencing of RNA isolated by cross-linking immunoprecipitation (HITS-CLIP), small-RNA-Seq, and mRNA-Seq data sets in Δ2A cells, making them a valuable resource for this study. Jurkat T and HEK293T cells were grown in RPMI 1640 and Dulbecco's modified Eagle's medium (DMEM) supplemented with 10% fetal bovine serum, 2 mM L-glutamine, and 100 U/ml penicillin-streptomycin.

HEK293T cells (about 70% confluent) were transfected with 100 pmol synthetic miRNAs using Lipofectamine 2000 (Life Technologies) in 6 wells and harvested 24 h posttransfection for Western blot analyses. About 1 million Jurkat T cells were nucleofected with 100 pmol synthetic miRNAs per cuvette using the 4D-Nucleofector SE cell line kit (program CL-120) from Lonza. The cells were harvested 24 h posttransfection for Western blot analyses. About 10 million HVS-infected marmoset T cells were nucleofected with 100 pmol synthetic miRNAs or 100 pmol locked nucleic acid (LNA) inhibitors per cuvette using the 4D-Nucleofector SE cell line kit (program CM-138) from Lonza. The transfected cells were then harvested 24 h posttransfection for Western blot analyses and cell counting.

Ago HITS-CLIP. About 5 million Δ2A cells were cross-linked with 600 mJ/cm^2 UV light (254 nm) on ice, lysed, and digested with RNase A. Ago HITS-CLIP was performed in four replicates using two anti-Ago antibodies (clones 2A8 and 11A9, each in duplicate), as described previously (4). The cDNA libraries were sequenced (using 50-cycle runs) by the Yale Stem Cell Center Genomics Core; about 100 million to 250 million reads were obtained per library. The data sets obtained previously (4) were reanalyzed to identify targets for miR-HSURs. High-quality raw sequencing reads were collapsed and selected for 7-mer (seed nucleotides 2 to 8) binding sites for miR-HSUR4-5p, miR-HSUR4-3p, miR-HSUR5-5p, and miR-HSUR5-5p. The reads containing seed binding sites for the miR-HSURs and the total reads were mapped to the reference marmoset genome (caljac 3.2) or HVS genome (NCBI reference sequence NC_001350.1) with Bowtie (10). A maximum of two mismatches were allowed for the alignment. Uniquely aligned reads were then collapsed according to their genomic coordinates unless the reads mapping to the same coordinate had unique degenerate barcodes. This step is important to eliminate PCR duplications, and the resulting uniquely mapped reads were referred to as Ago-bound mRNA fragments. Overlapping Ago-bound mRNA fragments were assembled into Ago clusters. Seed binding sites of host miRNAs (i.e., the top 100 most highly expressed in Δ2A cells) were searched for within miR-HSUR clusters to ensure that these clusters represent viral miRNA, not host miRNA, binding sites. Elimination of PCR duplication and Ago cluster assembly were performed using custom tools on Robert Darnell's laboratory server (Rockefeller University). To access the robustness of miR-HSUR-Ago clusters, the reproducibility (biological complexity [BC], as described in Results) and number of Ago-bound mRNA fragments (peak height [PH], as described in Results) in each individual experiment were used to determine a chi-square score for each cluster; a *P* value was then calculated from the chi-square score according to the method of Darnell et al. (11). Ago-bound mRNA fragments and Ago clusters were visualized on the University of California, Santa Cruz (UCSC), genome browser (http://genome.ucsc.edu). Cross-linking-induced mutations were analyzed according to the method of Zhang and Darnell (12).

GO analyses. Gene ontology (GO) analysis was done using DAVID Bioinformatics Resources (https://david.ncifcrf.gov). A total of 47 unique mRNAs containing statistically significant miR-HSUR-Ago clusters ($P \leq 0.05$, BC ≥ 3, and PH ≥ 10) in their 5′ untranslated regions (UTRs), 3′ UTRs, or coding sequences (CDSs) were used as the query gene list. All transcripts expressed in Δ2A cells identified by mRNA-Seq (fragments per kilobase per million [FPKM] ≥ 1) were used as background.

Small-RNA-Seq and mRNA-Seq analysis. Total RNAs were extracted from Δ2A cells using TRIzol (Life Technologies). A small-RNA library was prepared and sequenced as described previously (6). Quantification of mature-miRNA levels was performed using miRDeep2 (13). Because of the high degree of similarity between marmosets and humans, human miRNAs (from http://www.mirbase.org/) were used as references to quantify host miRNA levels. A poly(A)$^+$ RNA library was prepared from Δ2A cells and sequenced by the Yale Center for Genomic Analysis. Raw data were processed and analyzed, and transcript levels were quantified as described previously (4).

Luciferase reporter assays. Full-length 3′ UTRs of the miR-HSUR target genes, including *CSRP1* (cysteine- and glycine-rich protein 1), *OSTF1* (osteoclast-stimulating factor 1), *HSPA5* (heat shock protein A5), and *WEE1*, were PCR amplified from genomic DNA of Δ2A cells and then inserted into the multiple-cloning site downstream of the luciferase *luc2* gene in the pmiRGLO vector (Promega). Mutant reporters were generated by site-directed mutagenesis using the QuikChange protocol (Stratagene). To create a pmiRGLO reporter containing the miR-HSUR4-3p binding site from *EP300* in the CDS of the luciferase gene, a DNA fragment containing the NheI and SalI sites (i.e., 5′-GCTAGCGAATTCGTC GAC-3′) was first inserted upstream of the TAA stop codon of the *luc2* gene using the QuikChange protocol. Then, four copies of the miR-HSUR4-3p binding sites in *EP300* mRNA were cloned into the NheI and SalI sites. The DNA oligonucleotides used for cloning are shown in Table S4 in the supplemental material.

HEK293T cells were grown in 24-well tissue culture plates and then transfected with 5 ng pmiRGLO reporter, 0.8 μg pBlueScript II, and 20 pmol synthetic miRNAs per well. Dual-luciferase assays were performed 24 h posttransfection on a GloMax-Multi+ Microplate Multimode Reader (Promega) following the manufacturer's protocol. The firefly luciferase reading was first normalized to the *Renilla* luciferase reading. The ratios of firefly luciferase to *Renilla* luciferase for reporters with inserts were normalized to that of an empty reporter. The standard deviation (SD) for each condition was calculated based on a minimum of three independent experiments. *P* values were calculated using Student's *t* test.

Antibodies for Western blot analysis. The primary antibodies used were anti-p300 (catalog number sc-585; Santa Cruz Biotechnology), anti-BiP (catalog number 3183; Cell Signaling), anti-WEE1 (catalog number 4936; Cell Signaling), anti-Cdk1 (catalog number 9112; Cell Signaling), anti-phospho-Cdk1 (catalog number 9111; Cell Signaling), anti-glyceraldehyde-3-phosphate dehydrogenase (GAPDH) (catalog number 2118; Cell Signaling), and anti-tubulin (catalog number CP06; Calbiochem). GAPDH and tubulin provided normalization controls. The data shown in the figures are representative of the results of at least two independent experiments.

Synthetic miRNAs and LNAs. Synthetic mature and star miRNAs (IDT) were annealed to generate miRNA duplexes containing a 5′ phosphate (only on the mature miRNA strand, as indicated by "/phosphate/") and a 2-nucleotide (nt) 3′ overhang according to the method of Tuschl (14). The control miRNA has a random sequence, and its seed (nt 2 to 8) sequence is not identical to the seed of any known human miRNAs in the miRBase (http://www.mirbase.org). The synthetic miRNA sequences were as follows: control mature, 5′-/phosphate/GUACACCUAGGUGGA UCCUCU-3′; control star, 5′-AGGAUCCACCUAGGUGUGCAG-3′; miR-HSUR5-3p mature, 5′-/phosphate/UUACAGCAGUGAGAGCGCU GCU-3′; miR-HSUR5-3p star, 5′-CAGCGCUCUCACUGCUGUGAAG-3′; miR-HSUR4-3p mature, 5′-/phosphate/UUUAUAGCAGUGGGCAA CACGU-3′; miR-HSUR4-3p star, 5′-GUGUUGCCCACUGCUAUAA AAG-3′; miR-HSUR4-5p mature. 5′-/phosphate/ACCGUGUUGCUAC AGCUAUAA-3′; miR-HSUR4-5p star, 5′-AUAGCUGUAGCAACACGG UAG-3′; EBV-miR-BART-13 mature, 5′-/phosphate/UGUAACUUGC CAGGGACGGCUGA-3′; EBV-miR-BART-13 star, 5′-/AGCCGUCC CUGGCAAGUUAGAGA-3′. All LNA inhibitors were designed and synthesized by Exiqon.

Accession number. Four Ago HITS-CLIP data sets and visualization files have been deposited in the National Center for Biotechnology Information Gene Expression Omnibus and are accessible through accession number GSE71806.

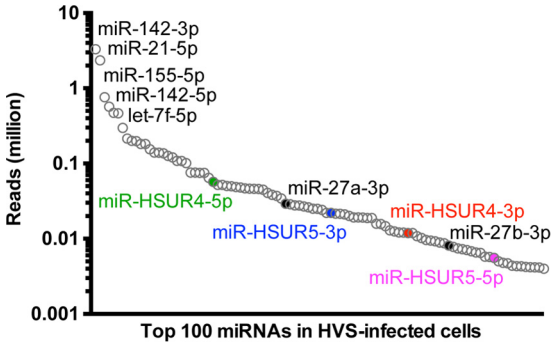

FIG 1 Mature-miR-HSUR levels determined by small-RNA-Seq analysis. The numbers of reads (million) for individual miRNAs are plotted for the top 100 most highly expressed host and viral miRNAs in HVS-infected marmoset T cells. Due to a deletion in the HVS genome (strain Δ2A), miR-HSUR2-5p and miR-HSUR2-3p are absent in these cells. The four HVS miRNAs are color coded as follows: miR-HSUR4-5p, green; miR-HSUR4-3p, red; miR-HSUR5-5p, magenta; and miR-HSUR5-3p, blue. A few relevant host miRNAs are also labeled.

RESULTS

Expression of miR-HSURs. To determine the levels of miR-HSURs in HVS-infected cells, we size selected small RNAs, constructed a cDNA library, and performed high-throughput sequencing (6). The sequencing data were quantified to determine relative levels of viral and host miRNAs. We were able to evaluate only four viral miRNAs—miR-HSUR4-5p, miR-HSUR4-3p, miR-HSUR5-5p, and miR-HSUR5-3p—because a deletion of the viral genome (the Δ2A deletion) removed DNA encoding miR-HSUR2-5p and miR-HSUR2-3p. Our results show that miR-HSURs are expressed at medium levels relative to the majority of cellular miRNAs (Fig. 1; see Table S1 in the supplemental material). The expression levels of miR-HSURs are similar to those of host miR-27a and miR-27b, which are known to play critical roles during HVS latency (3, 4). Homology searches showed that most miR-HSURs are not closely related to any annotated cellular or viral miRNAs, except for miR-HSUR5-5p, which is homologous to miR-937-3p.

Ago HITS-CLIP. To identify potential viral and host mRNAs targeted by miR-HSURs in Δ2A cells, we reanalyzed our Ago HITS-CLIP data sets (4), which were performed in four replicates using two different antibodies against Ago proteins, as described previously. Ago binding sites are represented by Ago clusters composed of overlapping Ago-bound mRNA fragments. Ago clusters containing binding sites for the seed (nt 2 to 8) sequences of miR-HSURs are referred to as miR-HSUR-Ago clusters.

miR-HSURs do not target viral mRNAs. First, we mapped the Ago HITS-CLIP data against the HVS genome to identify viral mRNAs targeted by miR-HSURs. As expected, we found that

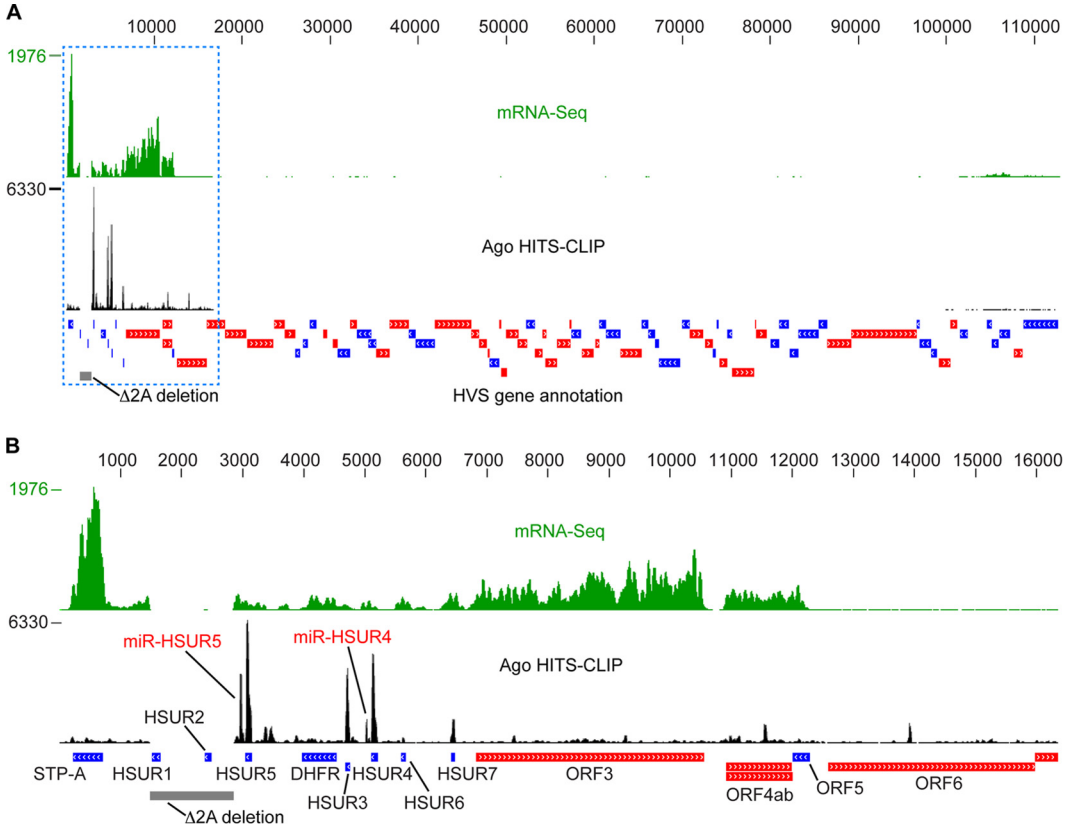

FIG 2 HVS latent gene expression and Ago binding sites. (A) mRNA-Seq and Ago HITS-CLIP reads were mapped to the HVS genome. HVS gene annotation is represented by the red (forward direction) and blue (reverse) rectangles. Note that only the left end of the viral genome is highly transcribed during latency, and this is where most Ago HITS-CLIP reads map. (B) Enlarged view of the left end of the HVS genome, boxed in blue in panel A. HVS genes are labeled as follows: STP-A, saimiri transforming protein A; DHFR, dihydrofolate reductase; ORF3, -4ab, -5, and -6, open reading frames 3, 4ab, 5, and 6. The Δ2A deletion is indicated by a gray bar. The mapped read number is shown on the *y* axis. Genomic coordinates are shown on top of panels A and B.

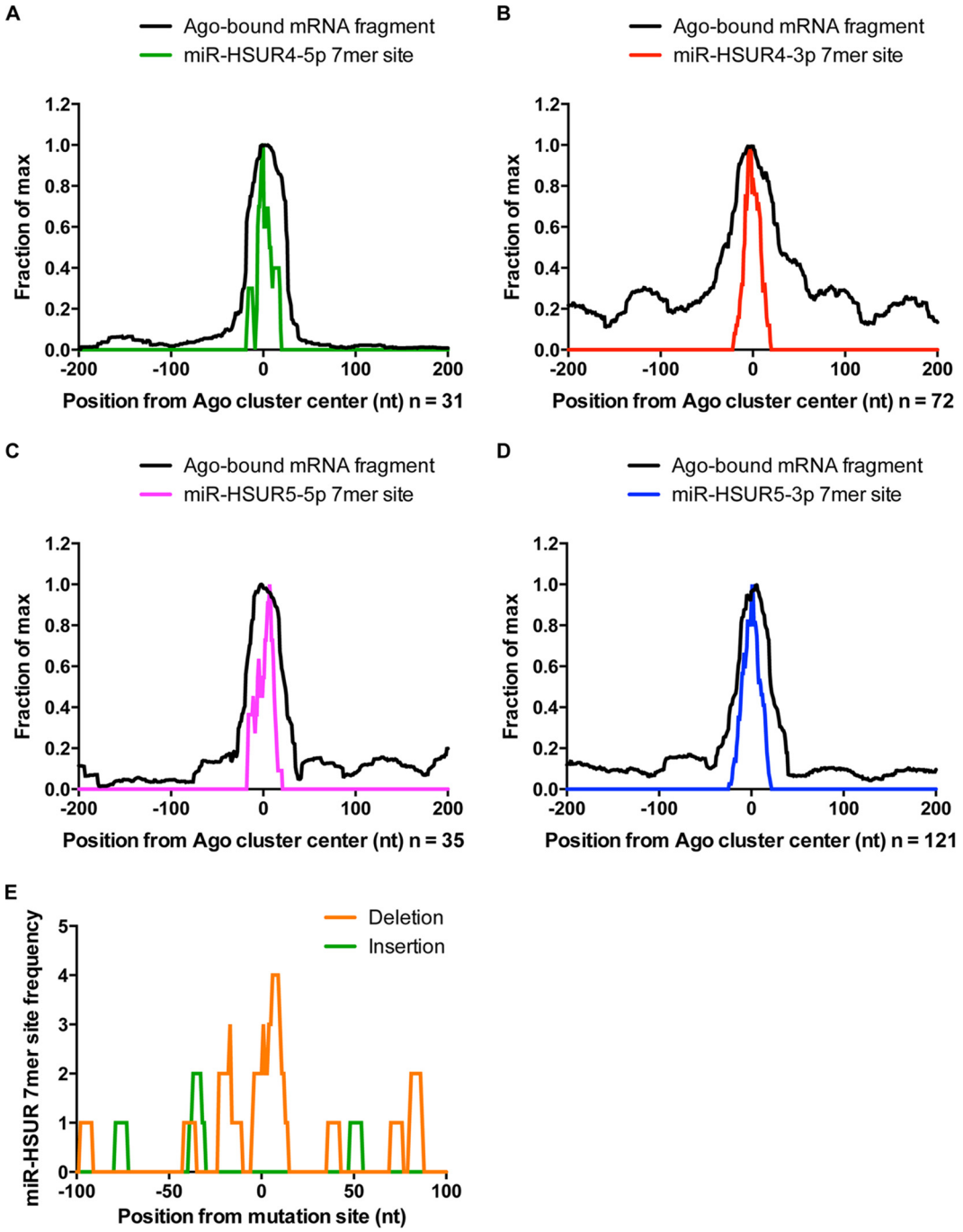

FIG 3 Metagene analyses of Ago clusters and 7-mer binding sites for miR-HSURs on the host genome. (A to D) Ago-bound mRNA fragments and 7-mer seed binding sites for each of the miR-HSURs were plotted relative to the centers (set to 0 nt) of miR-HSUR-Ago clusters (BC ≥ 3). The number of Ago clusters used in the metagene plots is shown for each miRNA. The distribution of seed binding sites for each viral miRNA is colored according to the scheme used in Fig. 1. (E) The frequencies of 7-mer seed binding sites for all four miR-HSURs are plotted relative to statistically significant (false discovery rate [FDR] < 0.001) cross-linking-induced mutation sites, including deletions and insertions. Insertions are not induced by Ago-mRNA cross-links (12), thus serving as a control.

miR-HSUR4-5p, miR-HSUR4-3p, miR-HSUR5-5p, and miR-HSUR5-3p associate with Ago (Fig. 2). Throughout the HVS transcriptome, Ago binding is highest on HSURs, including HSUR3, -4, -5, and -7, compared to other HVS RNAs (Fig. 2A). Because HSUR1 and -2 are known to base pair with host miRNAs and interact with Ago proteins, our data suggest that HSUR3, -4, -5, and -7 may interact with miRNAs, as well (2, 3). We found only a few Ago clusters mapping to viral mRNAs; this finding is consistent with low-level expression of a small number of HVS protein-coding genes during latency, as supported by mRNA-Seq analysis of poly(A)$^+$ RNA in Δ2A cells (Fig. 2A). Moreover, most of these Ago clusters do not contain sequences complementary to seed

nucleotides of miR-HSURs. The few miR-HSUR-Ago clusters mapping to the HVS genome are not statistically significant and therefore may represent background (see Table S2 in the supplemental material). We conclude that miR-HSURs do not significantly target viral mRNAs during latency.

Cellular mRNAs targeted by miR-HSURs. In contrast to the Ago binding profile on the HVS transcriptome, HITS-CLIP revealed many miR-HSUR-Ago clusters on the host transcriptome. We focused only on Ago clusters that were reproduced in at least three experiments (BC ≥ 3) and that contain 7-mer (seed nucleotides 2 to 8) binding sites for miR-HSURs. We found 31 miR-HSUR4-5p-Ago clusters, 72 miR-HSUR4-3p-Ago clusters, 35 miR-HSUR5-5p-Ago clusters, and 121 miR-HSUR5-3p-Ago clusters. To assess the quality of these clusters, we performed metagene analysis of the Ago-bound mRNA fragments and 7-mer (seed nucleotides 2 to 8) binding sites for each miR-HSUR (Fig. 3A to D). Our analysis revealed that the peaks of the two distributions overlap at the centers of the Ago clusters and that the width of the distribution for mRNA fragments is ~60 nt (Fig. 3A to D). These findings are consistent with previously reported miRNA-mediated Ago footprints on mRNAs (15). Furthermore, we found high frequencies of 7-mer (nt 2 to 8) binding sites for miR-HSURs near cross-linking-induced mutations in our HITS-CLIP data sets (Fig. 3E). This provides additional evidence that our experiment identified *in vivo* miRNA-mRNA interactions.

We then focused on the 75 most robust miR-HSUR-Ago clusters, defined by a BC of ≥3, a minimum of 10 Ago-bound mRNA fragments (PH ≥ 10), and a *P* value of ≤0.05 (see Table S3 in the supplemental material). Of these, 46% map to 3′ UTRs and 15% map to CDSs of annotated mRNAs (Fig. 4A). To determine the selectivity of our HITS-CLIP experiment, we plotted the PH of the Ago clusters against mRNA abundance (Fig. 4B). Because there is no correlation between the two variables, we conclude that the mRNA targets were specifically selected by HITS-CLIP. GO analyses showed that several pathways in cell cycle regulation are enriched among the top miR-HSUR targets (Fig. 4C), suggesting that miR-HSURs preferentially target cell cycle regulators. This is consistent with the T-cell oncogenic phenotype of HVS infection.

miR-HSUR4-3p targets *EP300* (p300). The most robust Ago cluster (PH = 296) identified in our HITS-CLIP data set mapped to the *EP300* mRNA (Fig. 5). Surprisingly, it resides within the CDS instead of the 3′ UTR of the mRNA. Within this Ago cluster, we identified an 8-mer (seed nucleotides 2 to 9) binding site for miR-HSUR4-3p. To test its activity, we inserted 4 in-frame copies of the binding site into the CDS of a luciferase reporter gene 6 nt upstream of the stop codon. As a control, identical sites were inserted into the 3′ UTR of the reporter. Transient cotransfection of the reporters with synthetic miR-HSUR4-3p or a control miRNA showed that this target site is active; point mutations that disrupt base-pairing interactions between miR-HSUR4-3p and the binding site abolish repression (Fig. 5A). The magnitude of miR-HSUR4-3p-mediated repression is larger when the target sites are in the 3′ UTR than when they are in the CDS of the reporter (Fig. 5A). By Western blotting, transient transfection of synthetic miR-HSUR4-3p into human HEK293T or Jurkat T cells reduced endogenous p300 protein levels compared to transfected control miRNAs (Fig. 5B and C; this binding site is conserved between marmosets and humans). In HVS-infected marmoset T cells, LNA inhibitor complementary to miR-HSUR4-3p increased p300 protein levels compared to control LNAs (Fig. 5D). Together, these

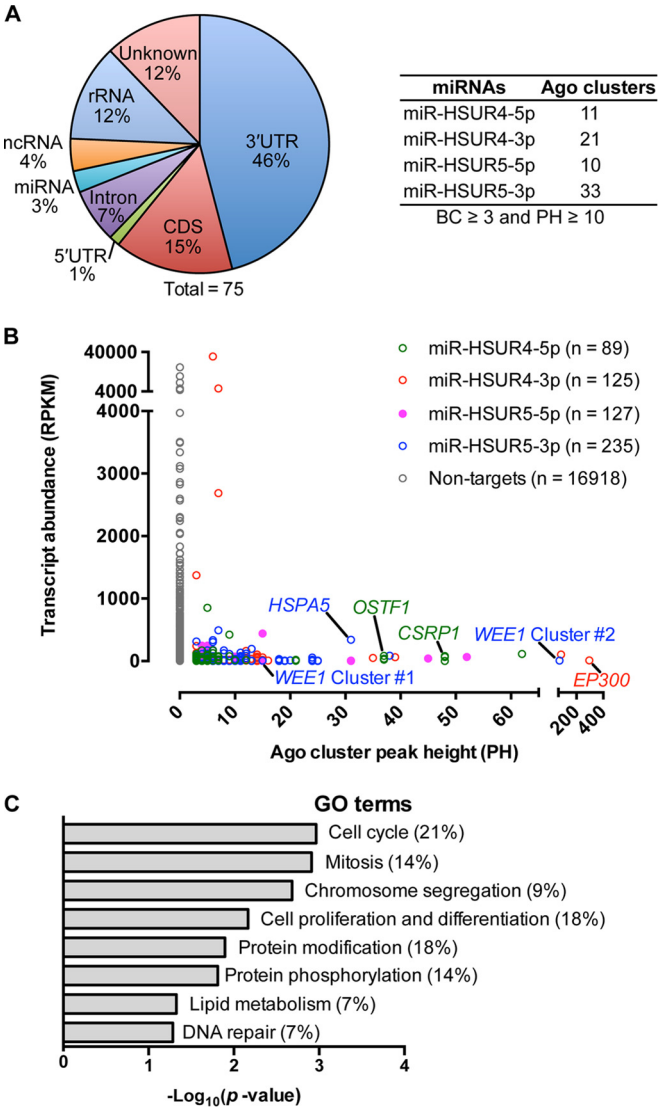

FIG 4 miR-HSURs preferentially target cell cycle regulators. (A) Genomic locations of the 75 statistically significant miR-HSUR-Ago clusters ($P \leq 0.05$, BC ≥ 3, and PH ≥ 10). ncRNA, noncoding RNA. (B) PH values for miR-HSUR-Ago clusters were plotted against transcript levels. (C) GO analysis reveals that HVS miRNAs target several pathways controlling cell cycle and proliferation. The percentage of viral miRNA targets in each pathway is indicated.

results show that p300 levels are repressed by HVS miR-HSUR4-3p via an interaction with a miRNA binding site in the CDS rather than in the 3′ UTR.

miR-HSUR4-5p targets *CSRP1* and *OSTF1*. Two robust miR-HSUR4-5p-Ago clusters mapped to the 3′ UTRs of cysteine- and glycine-rich protein 1 (*CSRP1*) and osteoclast-stimulating factor 1 (*OSTF1*) mRNAs (Fig. 6). The Ago cluster on *CSRP1* contains an 8-mer (seed nucleotides 2 to 9) binding site (Fig. 6A), and the cluster on *OSTF1* contains a 7-mer (seed nucleotides 2 to 8) binding site (Fig. 6B). We inserted the full-length 3′ UTR of *CSRP1* or *OSTF1* downstream of a luciferase reporter gene. Cotransfection of the reporters with synthetic miR-HSUR4-5p or a control miRNA showed that wild-type *CSRP1* and *OSTF1* 3′ UTRs elicited downregulation by miR-HSUR4-5p (Fig. 6). Mutations in the

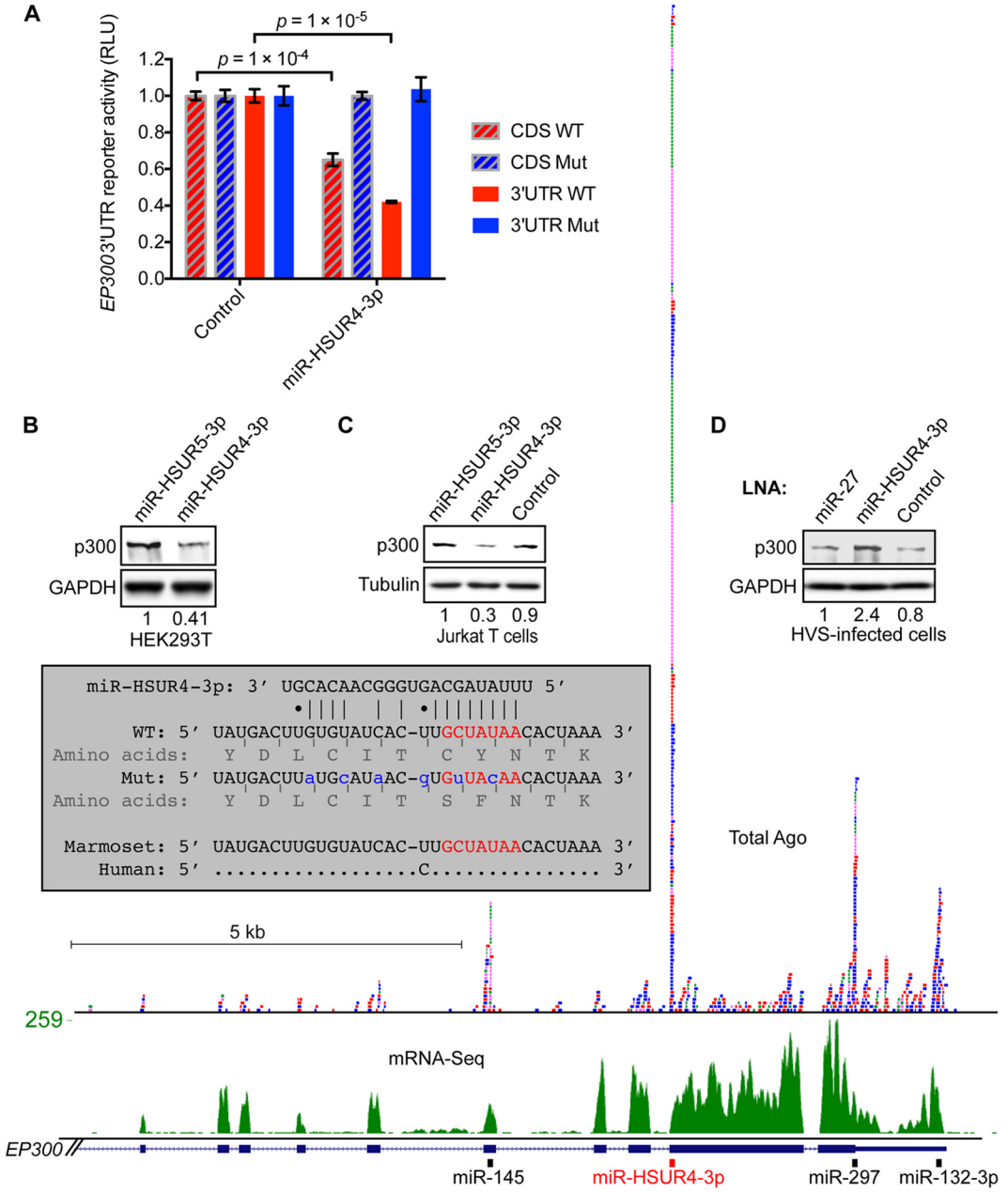

FIG 5 miR-HSUR4-3p regulates *EP300* via a target site in the CDS. (Bottom) Ago-bound mRNA fragments (from four replicates, marked with different colors), mRNA-Seq reads, and predicted miRNA target sites are mapped on the marmoset *EP300* mRNA (part of which is shown). (Box) Base-pairing interactions between miR-HSUR4-3p and wild-type (WT) (red) and mutant (Mut) (blue) binding sites used in the reporter assays in panel A are shown. Amino acids encoded by the WT and Mut target sites are also shown. Multiz alignment of genomic DNAs (http://genome.ucsc.edu/) of marmosets and humans for miR-HSUR4-3p target sites. Identical nucleotides are indicated by dots. (A) Luciferase reporter assays were performed with the WT or Mut 4× *EP300* CDS target site in HEK293T cells transfected with miR-HSUR4-3p or a control miRNA. A single copy of the *EP300* target site in the CDS of a luciferase reporter was not active enough to give a significant signal in reporter assays (data not shown). RLU, relative luciferase units. The bars show mean values ± SD from at least three experiments. (B and C) Western blots of p300 protein levels in HEK293T or Jurkat cells transfected with miR-HSUR4-3p, miR-HSUR5-3p, or a control miRNA. (D) Western blot showing p300 protein levels in HVS-infected marmoset T cells 24 h after transfection with LNA inhibitors against miR-27a, miR-HSUR4-3p, and a negative control. *P* values were calculated by the Student *t* test.

seed binding sites abolished miRNA-mediated repression; Epstein-Barr virus (EBV) miR-BART-13, complementary to the mutated binding sites, repressed only the mutant reporters (Fig. 6). These results indicate that miR-HSUR4-5p targets *CSRP1* and *OSTF1*.

miR-HSUR5-3p represses *HSPA5* (BiP). We found a miR-HSUR5-3p-Ago cluster mapping to the mRNA encoding heat shock protein A5 (*HSPA5*), also known as binding immunoglobulin protein (BiP) (Fig. 7A). This cluster contains an 8-mer (seed nucleotides 1 to 8) binding site for miR-HSUR5-3p (Fig. 7A). Reporter assays and mutagenesis analyses confirmed that the *HSPA5* 3′ UTR is a target of miR-HSUR5-3p (Fig. 7B). Because

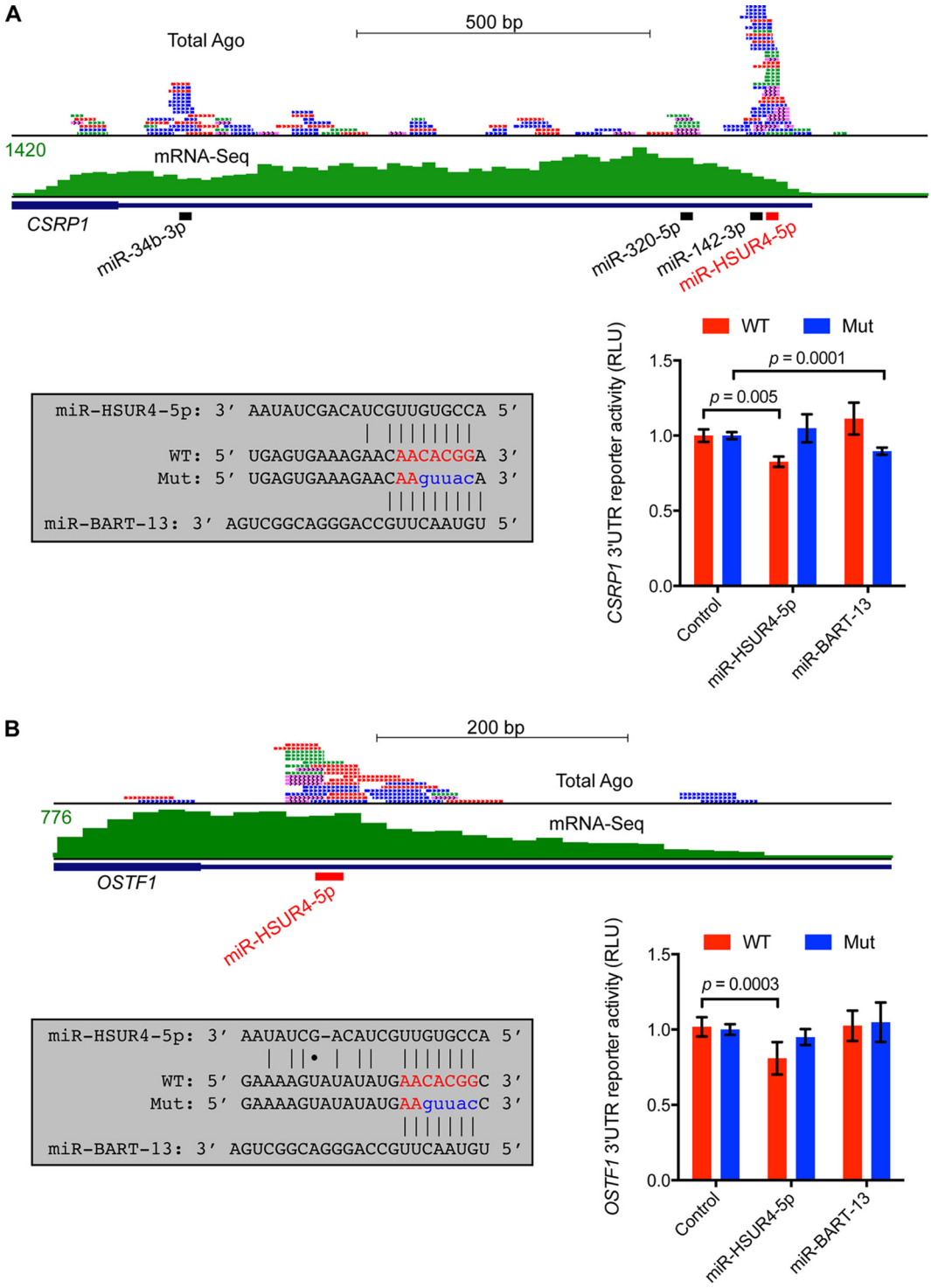

FIG 6 *CSRP1* and *OSTF1* are targeted by miR-HSUR4-5p. Ago-bound mRNA fragments, mRNA-Seq reads, and predicted miRNA target sites are mapped on the *CSRP1* (A) and *OSTF1* (B) 3′ UTRs as in Fig. 5. Validation of regulation by miR-HSUR4-5p was performed using luciferase reporter assays. Note that the mutant *OSTF1* 3′ UTR reporter was not repressed by EBV miR-BART-13, suggesting additional features or a requirement for factors in addition to the seed sequence. The bars represent means ± SD from at least three experiments. *P* values were calculated by the Student *t* test.

this target site is conserved between marmosets and humans, we transiently transfected synthetic miR-HSUR5-3p or a control miRNA into HEK293T or Jurkat T cells; Western blot analyses showed that endogenous BiP protein levels were reduced by miR-HSUR5-3p (Fig. 7C and D). In HVS-infected marmoset T cells, inhibition of miR-HSUR5-3p with a complementary LNA increased BiP protein levels (Fig. 7E). Our data therefore argue that miR-HSUR5-3p downregulates BiP in HVS-infected cells.

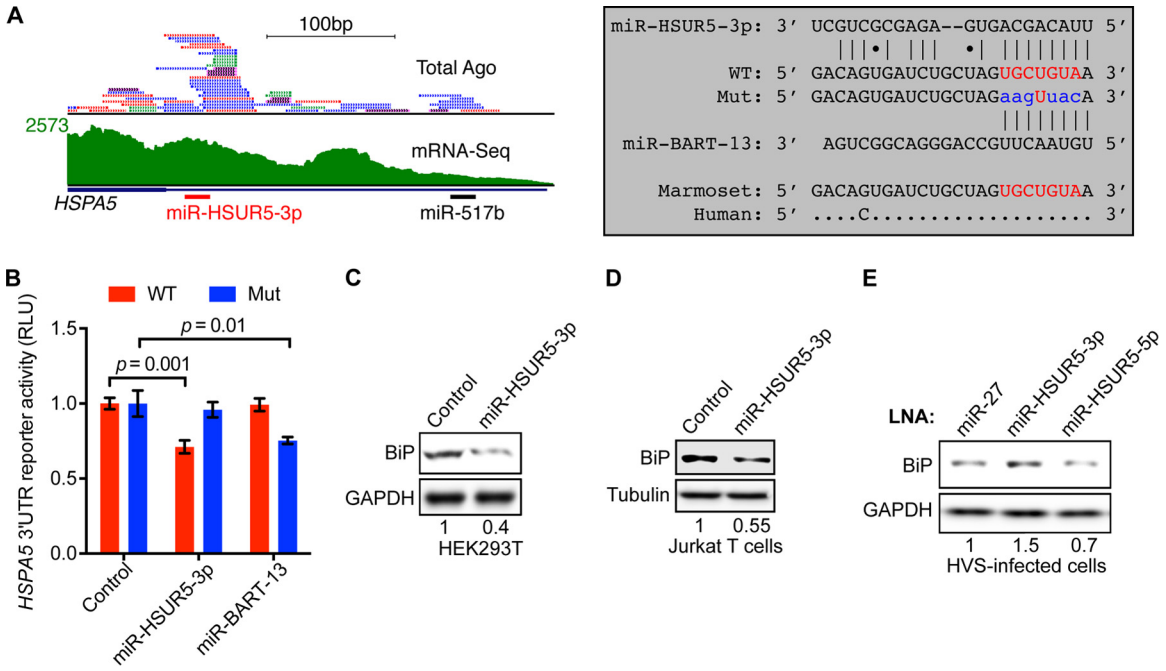

FIG 7 *HSPA5* is repressed by miR-HSUR5-3p. (A) Ago-bound mRNA fragments, mRNA-Seq reads, and predicted miRNA target sites mapped on the *HSPA5* 3′ UTR as in Fig. 5. Base-pairing interactions between the WT or Mut target site and miR-HSUR5-3p or miR-BART-13 are shown. Alignment of genomic DNAs of marmoset and human is shown for the miR-HSUR5-3p target sites as in Fig. 5. (B) Luciferase reporter assays were performed with the full-length WT or Mut *HSPA5* 3′ UTR and miR-HSUR5-3p, miR-BART-13, or a control miRNA. (C and D) Western blot analyses of BiP protein levels in HEK293T or Jurkat cells transfected with miR-HSUR5-3p or a control miRNA. (E) BiP levels 24 h after inhibition of miR-HSUR5-3p by the LNA inhibitor in HVS-infected cells. The bars represent mean values ± SD in at least three experiments. *P* values were calculated by the Student *t* test.

miR-HSUR5-3p targets *WEE1*. We found two robust miR-HSUR5-3p-Ago clusters on the 3′ UTR of *WEE1* mRNA, which contain an 8-mer (seed nucleotides 1 to 8) and a 7-mer (seed nucleotides 2 to 8) binding site, respectively (Fig. 8A). Using luciferase reporter assays and mutational analyses, we showed repression for the full-length wild-type 3′ UTR of *WEE1* upon transfection of synthetic miR-HSUR5-3p compared to control miRNAs; the mutant reporter was not repressed by miR-HSUR5-3p but was repressed by EBV miR-BART-13 (Fig. 8B). Transfection of miR-HSUR5-3p decreased endogenous WEE1 protein levels in both HEK293T and Jurkat T cells compared to a control miRNA (Fig. 8C and D, top) (note that both sites are conserved between marmosets and humans). Phosphorylation of cyclin-dependent kinase (Cdk1, also known as CDC2, a substrate of WEE1 kinase) was decreased upon transfection of miR-HSUR5-3p, whereas total Cdk1 levels were unchanged (Fig. 8C and D, bottom). Importantly, transfection of an LNA inhibitor complementary to miR-HSUR5-3p increased the protein level of WEE1 in HVS-infected T cells compared to control LNAs (Fig. 8E). Inhibition of miR-HSUR5-3p also led to a decrease in the number of HVS-infected cells (Fig. 8F).

DISCUSSION

Using Ago HITS-CLIP, we have identified mRNA targets for miR-HSURs in HVS-infected marmoset T cells. Unlike many other herpesviral miRNAs, which often regulate key latent viral proteins (2), miR-HSURs do not appear to target viral mRNAs in latently infected T cells (Fig. 2). This is not surprising, because the most abundant viral transcripts expressed by HVS in these cells are not mRNAs but the HSURs. However, it is possible that miR-HSURs may target leaky lytic transcripts present during latency and that these interactions might be below the detection limit of the methods employed in this study. Whereas miR-HSURs do not target viral mRNAs, they repress many host mRNAs, preferentially those encoding cell cycle regulators (Fig. 4C). Specifically, we discovered that miR-HSUR4-3p downregulates p300 via a binding site in the CDS of the *EP300* mRNA (Fig. 5) and that miR-HSUR5-3p directly decreases BiP and WEE1 protein production via binding sites in the 3′ UTRs of their mRNAs (Fig. 7 and 8). We also found that miR-HSUR5-3p decreases WEE1-mediated Cdk1 phosphorylation, which is required for normal growth of infected cells (Fig. 8). These results reveal functions of the miR-HSURs in HVS-infected T cells.

We also found that miR-HSUR4-5p targets *CSRP1* and *OSTF1* in HVS-infected cells (Fig. 6). *CSRP1* (also known as *CRP1*) is involved in transcription regulation during development, and reduced expression of *CSRP1* has been reported in human cancers (16, 17). On the other hand, *OSTF1* (also known as *SH3P2*) interacts with the Casitas B lineage lymphoma (*Cbl*) proto-oncogene and is involved in the tyrosine kinase Src signaling pathway (18, 19). Because the functions of *CSRP1* and *OSTF1* in T cells are not known, it is currently not clear why HVS represses these genes using viral miRNAs.

p300 is a transcription coactivator and histone acetyltransferase that has important functions in cell growth, transformation, and development (20). Many viral oncoproteins, including adenovirus E1A, simian virus 40 T antigen, human papillomavirus E6, Kaposi's sarcoma-associated herpesvirus vIRF, Epstein-Barr virus EBNA2, and polyomavirus large T antigen, are known to

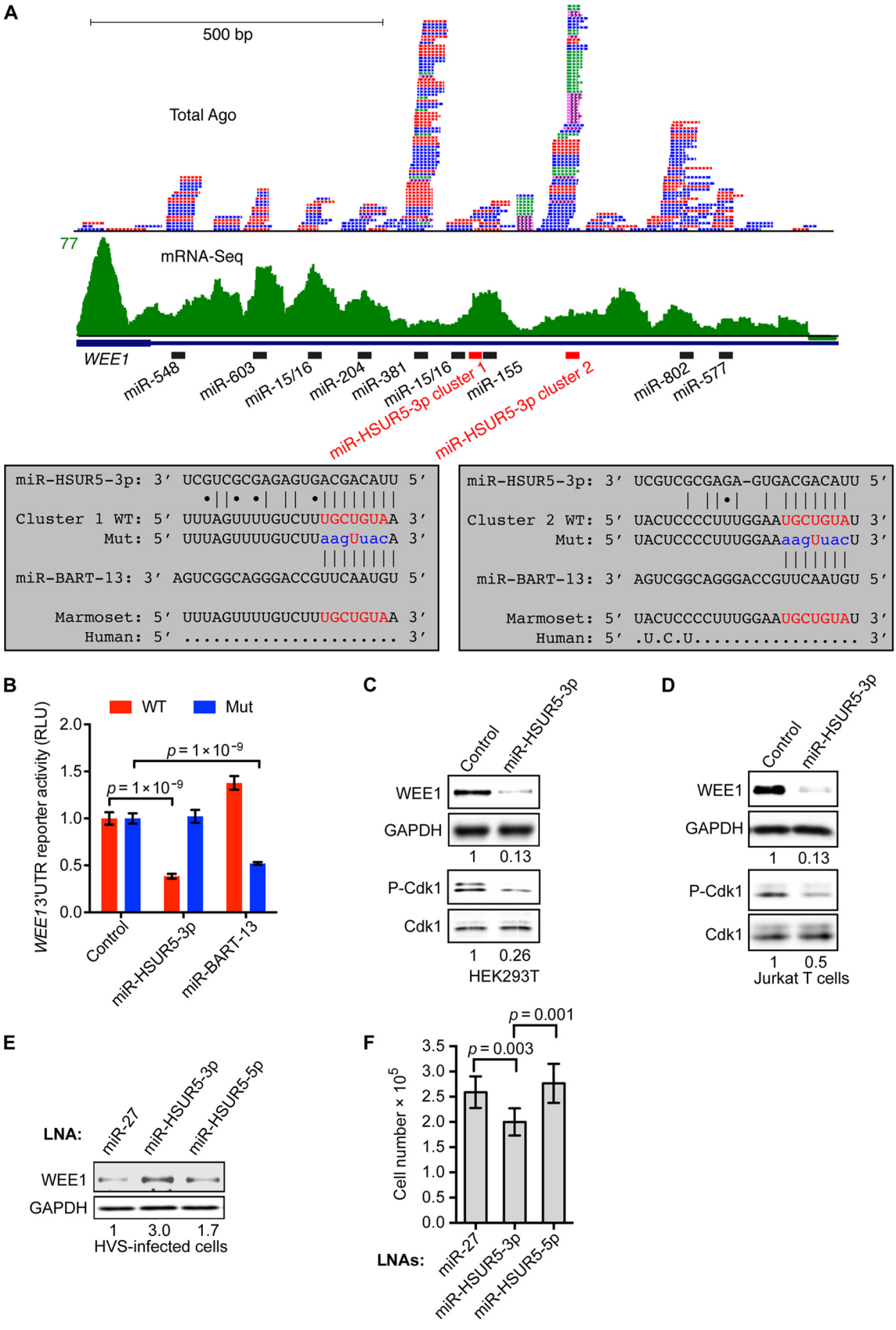

FIG 8 *WEE1* is a target of miR-HSUR5-3p. (A) Ago-bound mRNA fragments, mRNA-Seq reads, and predicted miRNA target sites mapped on the *WEE1* 3′ UTR as in Fig. 5. Alignment of genomic DNAs of marmoset and human is shown for miR-HSUR5-3p target sites as in Fig. 5. (B) Luciferase reporter assays were performed with the full-length WT or Mut *WEE1* 3′ UTR as described for Fig. 7. (C and D) Western blot analyses of the WEE1 protein and phosphorylated Cdk1 (P-Cdk1) from HEK293T or Jurkat cells transfected with miR-HSUR5-3p or a control miRNA. (E) WEE1 levels after inhibition of miR-HSUR5-3p by an LNA inhibitor in HVS-infected cells. (F) Numbers of HVS-infected cells 24 h after transfection of LNAs against miR-27a, miR-HSUR5-3p, or miR-HSUR5-5p. The bars show means ± SD from at least three experiments. *P* values were calculated by the Student *t* test.

interact with p300. Through these interactions, some viruses block various p300 activities, while others redirect p300 to regulate a different set of host genes. Thus, viruses employ p300 to play key roles in virus-induced cellular transformation and the viral life cycle (20, 21). Unlike other viruses, which utilize their protein products to modulate the activity of p300, HVS uses miR-HSUR4-3p to directly reduce p300 levels through base-pairing interactions with the CDS of the *EP300* mRNA (Fig. 5). Although overall there are fewer miRNA target sites in CDSs than in the 3′ UTRs of mRNAs (Fig. 4A), sites in other CDSs are conserved and appear functional (7, 22). Comparison of reporter repression mediated by the same p300 binding site located either in the CDS or the 3′ UTR shows that the CDS site confers less miRNA-mediated repression (Fig. 5A). However, our data cannot rule out the possibility that other factors might also contribute to robust Ago binding at this CDS site. For example, circular RNAs can form base-pairing interactions with miRNAs and modulate miRNA activity by functioning as a sponge to compete for target binding (17, 18). It is therefore possible that circular RNAs (circRNAs) generated from the *EP300* locus may base pair with miR-HSUR4-3p and contribute to miR-HSUR4-3p-Ago clusters (Fig. 5). To test this possibility, in circBase (http://www.circbase.org/) we identified 28 marmoset homologs of predicted human circRNAs produced from the *EP300* locus. We found no circRNA overlaps with the miR-HSUR4-3p-Ago cluster, suggesting that circRNAs are not likely contributors to this Ago cluster.

Our data reveal that BiP levels are directly regulated by miR-HSUR5-3p via an 8-mer binding site in the 3′ UTR (Fig. 7). BiP is an endoplasmic reticulum (ER)-localized HSP70 family chaperone that facilitates the proper folding of the major histocompatibility complex class I (MHC-I) protein complex (23). Because MHC-I plays key roles in the host immune response against viral infection, viruses have evolved strategies to downregulate MHC-I levels or to inhibit MHC-I function (24). Cancer cells also downregulate cell surface MHC-I levels in order to escape immune surveillance (25). In addition, secreted BiP has been found to elicit antitumor immunity (26). Thus, miR-HSUR5-3p-mediated reduction in BiP levels in HVS-infected cells might assist both immune evasion and viral transformation.

WEE1 kinase inhibits cell cycle progression by phosphorylating Cdk1, thereby preventing the G_2/M transition (27, 28). Because of its important role in cell growth and proliferation, WEE1 expression is tightly controlled at many levels; dysregulation of WEE1 leads to various diseases, including cancer (29). The *WEE1* mRNA is targeted by several miRNAs, including the well-known oncogenic miR-155 (30–32). Because overexpression of miR-155 is sufficient to cause cancers, miR-155-mediated downregulation of WEE1 is believed to contribute to oncogenesis (30). We discovered two robust miR-HSUR5-3p target sites in the 3′ UTR of *WEE1* mRNA. Using miR-HSUR5-3p, HVS decreases WEE1 kinase levels in infected cells, causing a decrease in the phosphorylated form of Cdk1 (Fig. 8). The unphosphorylated form of Cdk1 is active, promoting cell cycle progression, together with its partner proteins (27). Perhaps miR-HSUR5-3p enhances HVS-induced cell proliferation by downregulating WEE1. Consistent with this idea, inhibition of miR-HSUR5-3p by a complementary LNA leads to an increase in WEE1 protein and a decrease in the number of HVS-infected cells (Fig. 8F).

To explore the possible contributions of host miRNA binding to miR-HSUR-Ago clusters on *EP300*, *HSPA5*, and *WEE1*, we searched for potential base-pairing interactions with 7-mer seed nucleotides 2 to 8 of all host miRNAs (the top 100 most highly expressed in Δ2A cells) within these clusters. The miR-HSUR-Ago clusters do not contain seed binding sites for annotated host miRNAs. However, because of frequent heterogeneity at their 5′ ends, different isoforms of some host miRNAs may contribute to Ago binding at some miR-HSUR-Ago clusters. For example, we found that the miR-HSUR4-3p-Ago cluster on *EP300* (Fig. 5) can base pair with the seed (nt 2 to 8) of the miR-142-3p isoform, which is 1 nt shorter at the 5′ end. This binding site partially overlaps the miR-HSUR4-3p site, suggesting that the miR-142-3p isoform might also contribute to Ago binding. Similarly, miR-103/107 isoforms, also 1 nt shorter at their 5′ ends, can form seed (nt 2 to 8) base-pairing interactions (with a partially overlapping binding site for miR-HSUR5-3p) within the miR-HSUR5-3p-Ago cluster number 2 on the *WEE1* 3′ UTR. Viruses have evolved strategies to boost repression of some host mRNAs to benefit infection (5). For example, several oncogenic herpesviruses express homologs of host miR-155; these viral miRNAs share the seed sequence with miR-155 and downregulate the same set of targets (5). Perhaps miR-HSURs boost repression of key host genes important for HVS through seed binding sites that overlap some host miRNA isoforms. Viral miRNAs might exploit the existing host miRNA binding sites as an evolutionary shortcut to modulate host cell gene expression.

Our study has uncovered a new miRNA-based strategy used by HVS to control host gene expression during latency. These findings advance our understanding of the oncogenic strategy employed by herpesviruses.

ACKNOWLEDGMENTS

We thank Robert Darnell and members of the Darnell laboratory for their help with the HITS-CLIP analysis. We thank Kazimierz Tycowski and other members of the Steitz laboratory for helpful discussions and critical comments on the project, Demian Cazalla for sharing the small-RNA sequencing data from Δ2A cells, and Angela Miccinello for editorial assistance.

This work was supported by grant CA16038 from the NIH. J.A.S is an investigator at the Howard Hughes Medical Institute.

The content is solely our responsibility and does not necessarily represent the official views of the NIH.

REFERENCES

1. **Ensser A, Fleckenstein B.** 2005. T-cell transformation and oncogenesis by gamma2-herpesviruses. Adv Cancer Res **93:**91–128. http://dx.doi.org/10.1016/S0065-230X(05)93003-0.
2. **Tycowski KT, Guo YE, Lee N, Moss WN, Vallery TK, Xie M, Steitz JA.** 2015. Viral noncoding RNAs: more surprises. Genes Dev **29:**567–584. http://dx.doi.org/10.1101/gad.259077.115.
3. **Cazalla D, Yario T, Steitz JA.** 2010. Down-regulation of a host microRNA by a Herpesvirus saimiri noncoding RNA. Science **328:**1563–1566. http://dx.doi.org/10.1126/science.1187197.
4. **Guo YE, Riley KJ, Iwasaki A, Steitz JA.** 2014. Alternative capture of noncoding RNAs or protein-coding genes by herpesviruses to alter host T cell function. Mol Cell **54:**67–79. http://dx.doi.org/10.1016/j.molcel.2014.03.025.
5. **Guo YE, Steitz JA.** 2014. Virus meets host microRNA: the destroyer, the booster, the hijacker. Mol Cell Biol **34:**3780–3787. http://dx.doi.org/10.1128/MCB.00871-14.
6. **Cazalla D, Xie M, Steitz JA.** 2011. A primate herpesvirus uses the integrator complex to generate viral microRNAs. Mol Cell **43:**982–992. http://dx.doi.org/10.1016/j.molcel.2011.07.025.
7. **Bartel DP.** 2009. MicroRNAs: target recognition and regulatory functions. Cell **136:**215–233. http://dx.doi.org/10.1016/j.cell.2009.01.002.

8. **Skalsky RL, Cullen BR.** 2010. Viruses, microRNAs, and host interactions. Annu Rev Microbiol **64:**123–141. http://dx.doi.org/10.1146/annurev.micro.112408.134243.
9. **Cook HL, Lytle JR, Mischo HE, Li MJ, Rossi JJ, Silva DP, Desrosiers RC, Steitz JA.** 2005. Small nuclear RNAs encoded by Herpesvirus saimiri upregulate the expression of genes linked to T cell activation in virally transformed T cells. Curr Biol **15:**974–979. http://dx.doi.org/10.1016/j.cub.2005.04.034.
10. **Langmead B, Trapnell C, Pop M, Salzberg SL.** 2009. Ultrafast and memory-efficient alignment of short DNA sequences to the human genome. Genome Biol **10:**R25. http://dx.doi.org/10.1186/gb-2009-10-3-r25.
11. **Darnell JC, Van Driesche SJ, Zhang C, Hung KY, Mele A, Fraser CE, Stone EF, Chen C, Fak JJ, Chi SW, Licatalosi DD, Richter JD, Darnell RB.** 2011. FMRP stalls ribosomal translocation on mRNAs linked to synaptic function and autism. Cell **146:**247–261. http://dx.doi.org/10.1016/j.cell.2011.06.013.
12. **Zhang C, Darnell RB.** 2011. Mapping in vivo protein-RNA interactions at single-nucleotide resolution from HITS-CLIP data. Nat Biotechnol **29:**607–614. http://dx.doi.org/10.1038/nbt.1873.
13. **Friedlander MR, Mackowiak SD, Li N, Chen W, Rajewsky N.** 2012. miRDeep2 accurately identifies known and hundreds of novel microRNA genes in seven animal clades. Nucleic Acids Res **40:**37–52. http://dx.doi.org/10.1093/nar/gkr688.
14. **Tuschl T.** 2006. Annealing siRNAs to produce siRNA duplexes. CSH Protoc **2006:**pdb.prot4340. http://dx.doi.org/10.1101/pdb.prot4340.
15. **Chi SW, Zang JB, Mele A, Darnell RB.** 2009. Argonaute HITS-CLIP decodes microRNA-mRNA interaction maps. Nature **460:**479–486. http://dx.doi.org/10.1038/nature08170.
16. **Chang DF, Belaguli NS, Iyer D, Roberts WB, Wu SP, Dong XR, Marx JG, Moore MS, Beckerle MC, Majesky MW, Schwartz RJ.** 2003. Cysteine-rich LIM-only proteins CRP1 and CRP2 are potent smooth muscle differentiation cofactors. Dev Cell **4:**107–118. http://dx.doi.org/10.1016/S1534-5807(02)00396-9.
17. **Hirasawa Y, Arai M, Imazeki F, Tada M, Mikata R, Fukai K, Miyazaki M, Ochiai T, Saisho H, Yokosuka O.** 2006. Methylation status of genes upregulated by demethylating agent 5-aza-2′-deoxycytidine in hepatocellular carcinoma. Oncology **71:**77–85.
18. **Reddy S, Devlin R, Menaa C, Nishimura R, Choi SJ, Dallas M, Yoneda T, Roodman GD.** 1998. Isolation and characterization of a cDNA clone encoding a novel peptide (OSF) that enhances osteoclast formation and bone resorption. J Cell Physiol **177:**636–645.
19. **Szymkiewicz I, Destaing O, Jurdic P, Dikic I.** 2004. SH3P2 in complex with Cbl and Src. FEBS Lett **565:**33–38. http://dx.doi.org/10.1016/j.febslet.2004.03.100.
20. **Goodman RH, Smolik S.** 2000. CBP/p300 in cell growth, transformation, and development. Genes Dev **14:**1553–1577.
21. **Ferrari R, Gou D, Jawdekar G, Johnson SA, Nava M, Su T, Yousef AF, Zemke NR, Pellegrini M, Kurdistani SK, Berk AJ.** 2014. Adenovirus small E1A employs the lysine acetylases p300/CBP and tumor suppressor Rb to repress select host genes and promote productive virus infection. Cell Host Microbe **16:**663–676. http://dx.doi.org/10.1016/j.chom.2014.10.004.
22. **Hausser J, Syed AP, Bilen B, Zavolan M.** 2013. Analysis of CDS-located miRNA target sites suggests that they can effectively inhibit translation. Genome Res **23:**604–615. http://dx.doi.org/10.1101/gr.139758.112.
23. **Paulsson K, Wang P.** 2003. Chaperones and folding of MHC class I molecules in the endoplasmic reticulum. Biochim Biophys Acta **1641:**1–12. http://dx.doi.org/10.1016/S0167-4889(03)00048-X.
24. **Hansen TH, Bouvier M.** 2009. MHC class I antigen presentation: learning from viral evasion strategies. Nat Rev Immunol **9:**503–513. http://dx.doi.org/10.1038/nri2575.
25. **Garcia-Lora A, Algarra I, Garrido F.** 2003. MHC class I antigens, immune surveillance, and tumor immune escape. J Cell Physiol **195:**346–355. http://dx.doi.org/10.1002/jcp.10290.
26. **Tamura Y, Hirohashi Y, Kutomi G, Nakanishi K, Kamiguchi K, Torigoe T, Sato N.** 2011. Tumor-produced secreted form of binding of immunoglobulin protein elicits antigen-specific tumor immunity. J Immunol **186:**4325–4330. http://dx.doi.org/10.4049/jimmunol.1004048.
27. **Domingo-Sananes MR, Kapuy O, Hunt T, Novak B.** 2011. Switches and latches: a biochemical tug-of-war between the kinases and phosphatases that control mitosis. Philos Trans R Soc Lond B Biol Sci **366:**3584–3594. http://dx.doi.org/10.1098/rstb.2011.0087.
28. **McGowan CH, Russell P.** 1993. Human Wee1 kinase inhibits cell division by phosphorylating p34cdc2 exclusively on Tyr15. EMBO J **12:**75–85.
29. **Do K, Doroshow JH, Kummar S.** 2013. Wee1 kinase as a target for cancer therapy. Cell Cycle **12:**3159–3164. http://dx.doi.org/10.4161/cc.26062.
30. **Tili E, Michaille JJ, Wernicke D, Alder H, Costinean S, Volinia S, Croce CM.** 2011. Mutator activity induced by microRNA-155 (miR-155) links inflammation and cancer. Proc Natl Acad Sci U S A **108:**4908–4913. http://dx.doi.org/10.1073/pnas.1101795108.
31. **Butz H, Liko I, Czirjak S, Igaz P, Khan MM, Zivkovic V, Balint K, Korbonits M, Racz K, Patocs A.** 2010. Down-regulation of Wee1 kinase by a specific subset of microRNA in human sporadic pituitary adenomas. J Clin Endocrinol Metab **95:**E181–E191. http://dx.doi.org/10.1210/jc.2010-0581.
32. **Lezina L, Purmessur N, Antonov AV, Ivanova T, Karpova E, Krishan K, Ivan M, Aksenova V, Tentler D, Garabadgiu AV, Melino G, Barlev NA.** 2013. miR-16 and miR-26a target checkpoint kinases Wee1 and Chk1 in response to p53 activation by genotoxic stress. Cell Death Dis **4:**e953. http://dx.doi.org/10.1038/cddis.2013.483.